Surface Chirality

DOI: 10.1002/ange.200800255

Emerging Solvent-Induced Homochirality by the Confinement of Achiral Molecules Against a Solid Surface**

Nathalie Katsonis, Hong Xu, Robert M. Haak, Tibor Kudernac, Željko Tomović, Subi George, Mark Van der Auweraer, Albert P. H. J. Schenning,* E. W. Meijer,* Ben L. Feringa,* and Steven De Feyter**

The unique handedness of chiral molecules affects chemical, physical, and biological phenomena.[1–3] While observed in solution for helical polymers and self-assembled stacks of molecules,[4–8] transmission of chiral information is particularly selective at ordered interfaces as a result of geometrical restrictions introduced by two-dimensional (2D) confinement.[9–18] Chiral amplification of enantiomerically enriched mixtures has been demonstrated either by chemical reactions at the air–water interface,[19] or upon self-assembly on solid surfaces.[20] Homochirality in achiral enantiomorphous monolayers can be realized by merging chiral modifiers in the monolayer[21] or by exposing monolayers to magnetic fields.[22] Alternatively, the potential role of solvents in amplification of chirality and emergence of homochirality at surfaces remains unexplored to date.

Herein we show how solvent-induced macroscopic chirality emerges within self-assemblies of achiral molecules on achiral surfaces. It is an exclusive surface-confined process, and as such it differs from "chiral-solvent-" or "chiral-guest-induced" chirality of supramolecular systems in solution.

To demonstrate that homochirality emerges at the interface between a chiral liquid and the surface of highly oriented pyrolytic graphite (HOPG), we selected a hydrogen-bonding achiral diamino triazine oligo-(*p*-phenylenevinylene) oligomer (A-OPV4T, Figure 1). The chiral analogue, ((*S*)-OPV4T, Figure 1), was recently shown to assemble exclusively in a counter-clockwise (CCW) hydrogen-bonded rosette motif at the liquid–solid interface, with 1-phenyloctane as the achiral solvent.[23,24] Molecular homochirality is expressed at the supramolecular level as a result of the 2D packing of the chiral rosette. The chiral solvent in the current study,

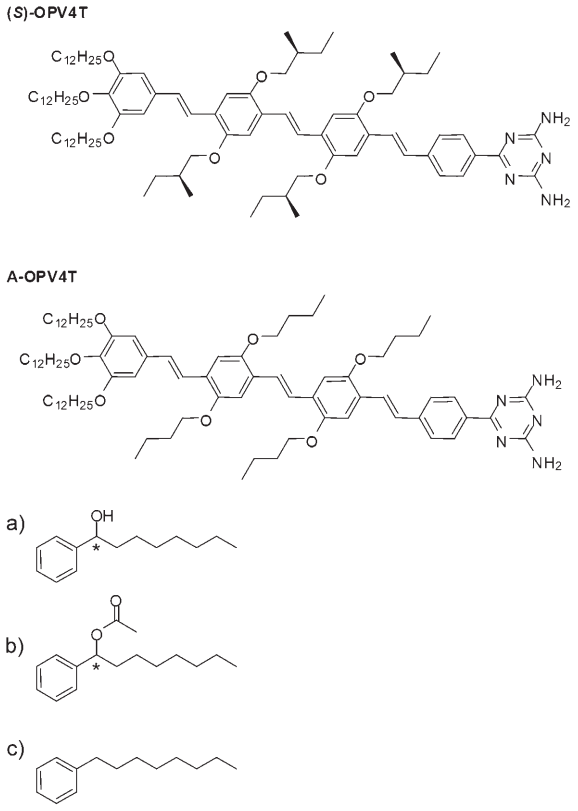

Figure 1. Molecular structures of the chiral ((*S*)-OPV4T) and achiral (A-OPV4T) 1,3-diamino triazine oligo-(*p*-phenylenevinylene) oligomers, synthesized according to established procedures. Solvents used in this study: a) 1-phenyl-1-octanol, b) 1-phenyl-1-octylacetate, c) 1-phenyloctane. The synthesis of these molecules is described in the Supporting Information.

[*] Dr. N. Katsonis,[+] R. M. Haak, Dr. T. Kudernac, Prof. B. L. Feringa
Stratingh Institute of Chemistry, University of Groningen
Nijenborgh 4, 9747 AG Groningen (The Netherlands)
Fax: (+31) 50-363-4296
E-mail: n.h.katsonis@rug.nl
b.l.feringa@rug.nl
Dr. Ž. Tomović, Dr. S. George, Dr. A. P. H. J. Schenning, Prof. E. W. Meijer
Laboratory for Macromolecular and Organic Chemistry
Eindhoven University of Technology
PO Box 513, 5600MB Eindhoven (The Netherlands)
Fax: (+31) 40-247-4706
E-mail: a.p.h.j.schenning@tue.nl
e.w.meijer@tue.nl
H. Xu, Dr. T. Kudernac, Prof. M. Van der Auweraer, Prof. S. De Feyter
Laboratory of Photochemistry and Spectroscopy and INPAC-Institute for Nanoscale Physics and Chemistry Katholieke Universiteit Leuven
Celestijnenlaan 200-F, 3001 Leuven (Belgium)
Fax: (+32) 1632-7990
E-mail: steven.defeyter@chem.kuleuven.be
[+] Current address: Centre d'Elaboration de Matériaux et d'Etudes Structurales, CNRS, BP 94347, 31055 Toulouse Cedex 4 (France)

[**] This work was supported by the Netherlands Organization for Scientific Research (NWO-CW) through a VENI (N. K.), a VIDI (A.S.), and a Spinoza (B.L.F.) grant, the Belgian Federal Science Policy Office through IAP-6/27, the Fund for Scientific Research—Flanders (FWO), and Marie Curie RTN CHEXTAN (MRTN-CT-2004-512161).

Supporting information for this article is available on the WWW under http://www.angewandte.org or from the author.

enantiomeric pure 1-phenyl-1-octanol (Figure 1),[25] represents the logical hybrid form between 1-phenyloctane and 1-octanol, solvents typically used for scanning tunneling microscopy (STM) imaging at the liquid–solid interface.[26–28] Furthermore, it was expected that 1-phenyl-1-octanol would be a good solvent, as it has the possibility to interact with the diaminotriazine moiety in A-OPV4T through hydrogen bonding.

The deposition of A-OPV4T from enantiomerically pure 1-phenyl-1-octanol onto a freshly cleaved surface of HOPG leads to the formation of monolayers covered by solvent. STM images show rosettes that are easily recognized as the star-shaped features with six bright arms (Figure 2). Each bright rod corresponds to a conjugated OPV backbone with its long molecular axis lying parallel to the surface. Alkyl chains are adsorbed in the low-contrast areas (Figure 2b and c). Close inspection of the STM images reveals that the rosettes are chiral: OPV units at opposite sites of the rosettes are not in line but show a clear non-radial orientation. Therefore, these rosettes can be classified into clockwise (CW) (Figure 2c) or counterclockwise (CCW; Figure 2b) rotating rosettes, the CW and CCW rosettes are mirror images of each other. Most importantly, from sets of large-scale images (such as the image shown in Figure 2a), it appears that, within the observed monolayer, there is a clear bias towards CCW rotating rosettes in (*R*)-1-phenyl-1-octanol and CW rotating rosettes in (*S*)-1-phenyl-1-octanol.

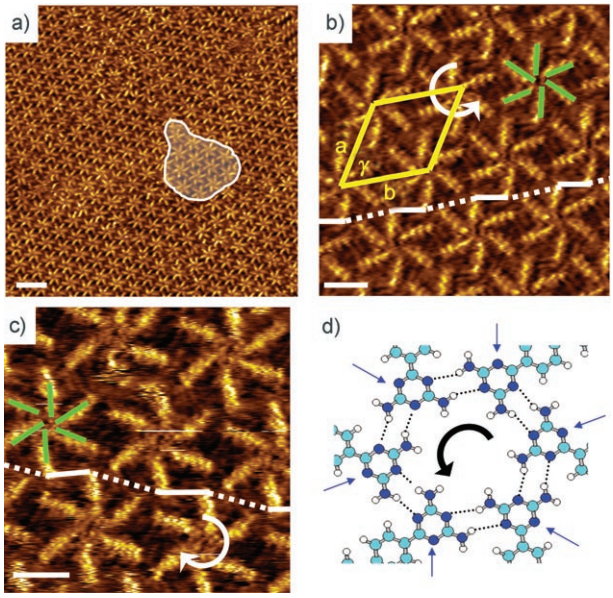

Figure 2. a) and b) STM images of an A-OPV4T monolayer at the (*R*)-1-phenyl-1-octanol–HOPG interface. a) In addition to several domains of CCW rosettes, one CW domain is observed as marked. Scale bar is 10 nm. b) High-resolution image of the CCW rosette. Individual OPV units are indicated by green lines emphasizing the non-radial orientation. The rotation direction is highlighted by the white arrow. Scale bar is 3 nm. Sequence of dashed and solid white marker lines from left to right: dashed-up and solid-down. c) Molecular resolution STM image of an A-OPV4T monolayer at the (*S*)-1-phenyl-1-octanol–HOPG interface. The CW rotation direction is highlighted by the white arrow. Scale bar is 3 nm. Sequence of dashed and solid white marker lines from left to right: dashed-down and solid-up. d) Anticipated hydrogen-bonding motif of the CCW rotating rosette, involving six A-OPV4T molecules. Blue arrows indicate the nitrogen atoms which remain free to interact by hydrogen bonding with the solvent molecules; dark blue N, light blue C, white H.

In addition to the expression of chirality at the level of the rosettes, the next level in their hierarchical self-assembly, that is, the relative orientation of the rosettes within the monolayer, is chiral and solvent-dependent too (note the sequence of the longer dashed and shorter solid white marker lines in Figure 2b and Figure 2c, which connect the terminal phenyl groups of similarly oriented OPV units along unit cell vector *b*. Their sequence and relative orientation highlight the chiral nature of the monolayer). In both enantiomeric pure solvents, many ordered domains of variable size were observed. Within a given domain, the rosettes are ordered in rows and form a homochiral crystalline lattice characterized by the following unit cell parameters which are within experimental error identical to those of (*S*)-OPV4T at the 1-phenyloctane–HOPG interface:[24] $a=(6.11\pm0.06)$ nm, $b=(6.13\pm0.04)$ nm, $\gamma=(60\pm1)°$ in (*S*)-1-phenyl-1-octanol (Figure 2c) and $a=(6.09\pm0.06)$ nm, $b=(6.04\pm0.05)$ nm, $\gamma=(62\pm2)°$ in (*R*)-1-phenyl-1-octanol (Figure 2b). A-OPV4T self-assembles into a chiral pattern in accordance with the plane group *p*6, which is one of the five chiral plane groups.[29,30]

To confirm solvent-induced asymmetric induction at the liquid–solid interface, a statistical analysis was performed indexing the individual rosettes as CW or CCW. This analysis was carried out by using several batches of solvent and substrates, and by probing more than a thousand rosettes for each experiment. The results show that monolayer formation in enantiomeric pure 1-phenyl-1-octanol solvents clearly leads to solvent-induced asymmetric induction (Table 1). A 100% asymmetry induction is never observed though, likely because of the slow kinetics of the ordering process. The measured enantiomeric ratios (CCW versus CW) range from 17 (CCW): 83 (CW) in (*S*)-1-phenyl-1-octanol to 91 (CCW): 9 (CW) in (*R*)-1-phenyl-1-octanol. These values are comparable within the experimental error.

To investigate the role of 1-phenyl-1-octanol, we have tested other solvents such as 1-phenyloctane, *rac*-1-phenyl-1-octane, (*R*)-1-phenyl-1-octylacetate and (*S*)-1-phenyl-1-octylacetate. The statistical analyses of sets of STM images do not reveal a significant bias of either CCW or CW rosettes in these cases (Table 1). These results demonstrate that hydrogen-bonding interactions between the enantiomeric pure 1-phenyl-1-octanol molecules and A-OPV4T are key in inducing surface homochirality.[31]

Circular dichroism (CD) measurements of A-OPV4T in either (*R*)- or (*S*)-1-phenyl-1-octanol were performed, using a typical STM concentration ($c=3\times10^{-5}$ mol L^{-1}). No CD effects were observed,[32] revealing that neither potential pre-formation of the rosettes nor formation of chiral assemblies are involved. The formation of rosettes exclusively at the liquid–solid interface is also shown by STM images recorded a few minutes after deposition on the surface, these images show disordered monolayers typically observed from achiral solvents. A solvent monolayer acting as a chiral template underneath the rosettes is unlikely because at room temperature, in the absence of the A-OPV4T molecules, deposition

Table 1: Asymmetric induction in A-OPV4T monolayers at various liquid–solid interfaces.[a]

Solvent	1) No. of rosettes analyzed 2) % of distinct rotating rosettes: CCW + CW	1) Enantiomeric ratio CCW:CW 2) (Stand.Dev.)
(*R*)-1-phenyl-1-octanol	2209 86	91:9 (9)
(*S*)-1-phenyl-1-octanol	1948 71	17:83 (14)
rac-1-phenyl-1-octanol	4190 78	54:46 (14)
(*R*)-1-phenyl-1-octyl acetate	1019 44	55:45 (15)
(*S*)-1-phenyl-1-octyl acetate	1194 42	48:52 (12)

[a] All STM images were registered at least one hour after deposition on the surface, to allow the monolayers to organize in view of the dynamics taking place. Typically, the waiting time was longer for *rac*-1-phenyl-1-octanol than for the corresponding enantiomeric pure solvent. A significant number of areas per solvent was probed: (*R*)-1-phenyl-1-octanol (16 areas), (*S*)-1-phenyl-1-octanol (17), *rac*-1-phenyl-1-octanol (52), (*R*)-1-phenyl-1-octyl acetate (13), (*S*)-1-phenyl-1-octyl acetate (15). The standard deviation of the weighted mean of the enantiomeric ratio (so corrected for the number of chiral rosettes per area) is given in parentheses. Note that the standard deviation for a constant number of probed rosettes should become smaller by scanning larger areas, which is limited though by the need for high spatial resolution.

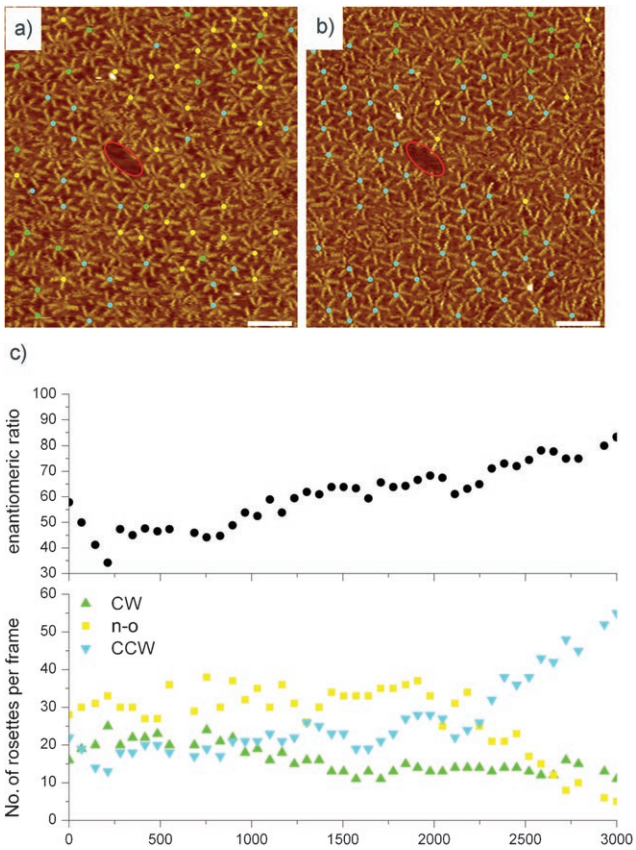

Figure 3. a) First and b) last frame of a sequence of STM images of an A-OPV4T monolayer at the (*R*)-1-phenyl-1-octanol–HOPG interface recorded at the same area. The time gap between the frames is 50 min. Scale bar is 10 nm. The center of the rosettes is color-coded: CCW (blue), CW (green), n-o (not-ordered) orientation (yellow). The red bordered dark defect area acts as a marker region. c) Evolution of the enantiomeric ratio (CCW/(CCW+CW)) and the number of rosettes of a given orientation (CCW, CW, or n-o orientation) as a function of time.

of (*R*)-1-phenyl-1-octanol or (*S*)-1-phenyl-1-octanol on HOPG never resulted in the observation of any ordered layer. In addition, the unit cell parameters of ordered rosette domains in the different solvents are identical, regardless if chiral induction is observed or not. Combined with the fact that the unit cell parameters are also identical to those of (*S*)-OPV4T, it is safe to conclude that solvent molecules are not co-adsorbed within the plane of the monolayer, that is, there are no solvent molecules between the rosettes.

STM at the liquid–solid interface not only allows the extent of chiral induction on the surface to be evaluated, but also enables how homochirality emerges to be observed (Figure 3). Therefore, we recorded series of STM images at the (*R*)-1-phenyl-1-octanol–HOPG interface over a period of 50 min (Video1 in the Supporting Information). For each frame, the number of CCW, CW rosettes, and ill-defined cyclic hexamers with no identifiable orientation (not-ordered (n-o)) have been measured and their evolution in time is indicated in Figure 3c, revealing a clear correlation between the appearance of order and the emergence of chirality. Over time, the number of CCW rosettes increases at the expense of those with no identifiable orientation (n-o) and, to a lesser extent, of the CW rosettes. In this time-dependent sequence, the enantiomeric ratio increases from about 50:50 CCW:CW to 80:20 CCW:CW after 50 min (Video1 in the Supporting Information). For the same sample, but at a different area, a similar sequence of images was recorded, but starting three hours later. In this case the initial enantiomeric ratio is already at a high level and doesn't change significantly in time (Video2 in the Supporting Information). This evolution from non-ordered rosettes to CCW or CW rosettes, or the evolution from CW rosettes into CCW rosettes (or vice versa), depending on the chirality of the solvent, was observed in all our experiments. As an example, Figure 4 shows the evolution of a CW rosette into a CCW rosette. The conversion of n-o rosettes to CW or CCW rosettes happens both at domain boundaries and in the bulk of the disordered domains. This conversion is not necessarily faster at domain boundaries but there the nature of the conversion (forming CW or CCW rosettes) is clearly dictated by the chirality of the ordered domain. Clearly, as a result of the confinement, in well-packed domains the conversion of CW into CCW rosettes (or vice versa) happens primarily at the domain boundaries. Similarly, the transition of other structures, such as dimers to rosette-type objects has also been identified.[32]

Multiple pathways to the emergence of homochirality coexist. Disorder–order transitions occur not only at the level of the individual rosettes but also at the monolayer level. It is hard to foresee how an isolated rosette will have preferred chirality because 2D crystallization also plays a role in the chiral selection: in the 2D lattice, the preference of a

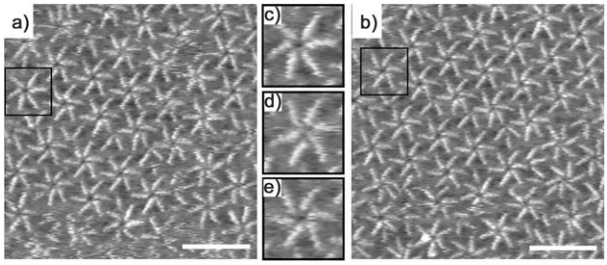

Figure 4. a) First and b) last frame of a sequence of STM images of an A-OPV4T monolayer at the (*R*)-1-phenyl-1-octanol–HOPG interface recorded at the same area. The time gap between the frames is 142 seconds. Scale bar is 10 nm. The area of interest is indicated by the black square. An enlargement of that area is shown in c) after 0 s, in d) after 95 s, and in e) after 142 s. Over time, the irregular cyclic hexamer indicated in the square evolves into a CCW rosette.

conglomerate 2D lattice over the racemic lattice will lead to the addition of small energy differences at the supramolecular level.

The actual mechanism of chiral selection that favors the formation of rosettes with a particular handedness during 2D crystallization is not known. It probably involves interactions between the solvent and the rosettes, chiral desolvation processes, steric restrictions within the monolayer—in which order is favored—or, most probably, an interplay of all these effects. The time dependence reflected in our experiments does not support a hypothesis of emergence of homochirality purely resulting from improved order and underlines the importance of additional kinetic effects. One possible scenario is that upon surface-mediated self-assembly, individual rosettes are formed. The unbound nitrogen atoms in these rosettes (Figure 2d) are likely to transiently interact through hydrogen bonding with the solvent molecules. In an achiral solvent, physisorption by desolvation leads to the disappearance of these complexes and the formation of physisorbed rosettes, without any favored handedness. However, we anticipate that the use of a chiral solvent favors the formation of transient complexes with a particular handedness. Upon desolvation, rosettes with a particular handedness are formed on the surface. The self-assembly of rosettes with the same handedness further improves the order within the monolayer.

In summary, we have shown that 2D crystallization at the interface between an achiral surface and a chiral solvent can produce enantiomerically enriched, and even homochiral organic surfaces. In other words, chirality on one scale (a stereocenter in a chiral solvent molecule) has been manifested on the larger scales of a surface-confined hierarchical supramolecular assembly. The demonstration of control of chirality on surfaces in synthetic achiral molecular systems by chiral solvents is a simple method and is of considerable interest for asymmetric synthesis, heterogeneous asymmetric catalysis, chiral separation, or the fabrication of advanced functional materials.

Experimental Section

STM experiments were performed at room temperature. Pt/Ir STM tips were prepared by mechanical cutting from Pt/Ir wire (80:20, diameter 0.25 mm). Prior to imaging, A-OPV4T or (*S*)-OPV4T molecules were dissolved in the solvents by sonication (few minutes) and heating at 40 °C (15 min). The solutions obtained had a concentration ranging between 10^{-4} to 10^{-5} M. Subsequently, a drop of the solution was applied to a freshly cleaved surface of HOPG, and then the STM tip was immersed into the drop. The system was then allowed to cool for at least 30 min before measuring.

Information on materials, synthesis and characterization of the chiral solvents, UV/Vis and CD spectroscopy experiments, complementary STM images and movies (Video1 and Video2) are collected in the Supporting Information.

Received: January 17, 2008
Revised: March 17, 2008
Published online: May 27, 2008

Keywords: chirality · liquid–solid interfaces · scanning probe microscopy · self-assembly · supramolecular chemistry

[1] a) L. Perez-Garcia, D. B. Amabilino, *Chem. Soc. Rev.* **2002**, *31*, 342–356; b) L. Perez-Garcia, D. B. Amabilino, *Chem. Soc. Rev.* **2007**, *36*, 941–967.
[2] M. Avalos, R. Babiano, P. Cintas, J. Jimenez, J. C. Palacios, L. D. Barron, *Chem. Rev.* **1998**, *98*, 2391–2404.
[3] B. L. Feringa, R. A. van Delden, *Angew. Chem.* **1999**, *111*, 3624–3645; *Angew. Chem. Int. Ed.* **1999**, *38*, 3418–3438.
[4] M. M. Green, C. Khatri, N. C. J. Peterson, *J. Am. Chem. Soc.* **1993**, *115*, 4941–4942.
[5] a) A. R. A. Palmans, J. A. J. M. Vekemans, E. E. Havinga, E. W. Meijer, *Angew. Chem.* **1997**, *109*, 2763–2765; *Angew. Chem. Int. Ed. Engl.* **1997**, *36*, 2648–2651; b) A. R. A. Palmans, E. W. Meijer, *Angew. Chem.* **2007**, *119*, 9106–9126; *Angew. Chem. Int. Ed.* **2007**, *46*, 8948–8968.
[6] H. von Berlepsch, S. Kirstein, C. Bottcher, *J. Phys. Chem. B.* **2003**, *107*, 9646–9654.
[7] K. Toyofuku, M. Akhtarul Alam, A. Tsuda, N. Fujita, S. Sakamoto, K. Yamaguchi, T. Aida, *Angew. Chem.* **2007**, *119*, 6596–6600; *Angew. Chem. Int. Ed.* **2007**, *46*, 6476–6480.
[8] S. J. George, Ž. Tomović, M. M. J. Smulders, T. F. A. de Greef, P. E. L. G. Leclère, E. W. Meijer, A. P. H. J. Schenning, *Angew. Chem.* **2007**, *119*, 8354–8359; *Angew. Chem. Int. Ed.* **2007**, *46*, 8206–8211.
[9] G. P. Lopinski, D. J. Moffatt, D. D. M. Wayner, R. A. Wolkow, *Nature* **1998**, *392*, 909–911.
[10] M. Ortega Lorenzo, C. J. Baddeley, C. Muryn, R. Raval, *Nature* **2000**, *404*, 376–379.
[11] A. Kühnle, T. R. Lindertoh, B. Hammer, F. Besenbacher, *Nature* **2002**, *415*, 891–893.
[12] Q. Chen, N. V. Richardson, *Nat. Mater.* **2003**, *2*, 324–328.
[13] Y. Wei, K. Kannappan, G. W. Flynn, M. B. Zimmt, *J. Am. Chem. Soc.* **2004**, *126*, 5318–5322.
[14] M. Lingenfelder, G. Tomba, G. Costantini, L. C. Ciacchi, A. De Vita, K. Kern, *Angew. Chem.* **2007**, *119*, 4576–4579; *Angew. Chem. Int. Ed.* **2007**, *46*, 4492–4495.
[15] N. Katsonis, A. Minoia, T. Kudernac, T. Mutai, H. Xu, H. Uji-i, R. Lazzaroni, S. De Feyter, B. L. Feringa, *J. Am. Chem. Soc.* **2008**, *130*, 386–387.
[16] N. Katsonis, E. Lacaze, B. L. Feringa, *J. Mater. Chem.* **2008**, *18*, 2065–2073.
[17] "Supramolecular surface chirality": K. H. Ernst, *Top. Curr. Chem.* **2006**, *269*, 209–252.
[18] S. De Feyter, F. C. De Schryver in *Scanning Probe Microscopies beyond Imaging: Manipulation of Molecules and Nanostructures*, Wiley-VCH, Weinheim, **2006**.

[19] H. Zepik, E. Shavit, M. Tang, T. R. Jensen, K. Kjaer, G. Bolbach, L. Leiserowitz, I. Weissbuch, M. Lahav, *Science* **2002**, *295*, 1266 – 1269.
[20] R. Fasel, M. Parschau, K.-H. Ernst, *Nature* **2006**, *439*, 449 – 452.
[21] M. Parschau, S. Romer, K.-H. Ernst, *J. Am. Chem. Soc.* **2004**, *126*, 15398 – 15399.
[22] A. M. Berg, D. L. Patrick, *Angew. Chem.* **2005**, *117*, 1855 – 1857; *Angew. Chem. Int. Ed.* **2005**, *44*, 1821 – 1823.
[23] P. Jonkheijm, A. Miura, M. Zdanowska, F. J. M. Hoeben, S. De Feyter, A. P. H. J. Schenning, F. De Schryver, E. W. Meijer, *Angew. Chem.* **2004**, *116*, 76 – 80; *Angew. Chem. Int. Ed.* **2004**, *43*, 74 – 78.
[24] A. Miura, P. Jonkheijm, S. De Feyter, A. P. H. J. Schenning, E. W. Meijer, F. C. De Schryver, *Small* **2005**, *1*, 131 – 137.
[25] The preparation method was modified and optimized from K. Mori, R. Bernotas, *Tetrahedron: Asymmetry* **1990**, *1*, 97 – 110 and the enantiomeric excess as measured by high-performance liquid chromatography was higher than 99 % (see methods in Supporting Information).
[26] J. P. Rabe, S. Buchholtz, *Science* **1991**, *253*, 424 – 427.
[27] D. M. Cyr, B. Venkataraman, G. W. Flynn, *Chem. Mater.* **1996**, *8*, 1600 – 1615.
[28] W. Mamdouh, H. Uji-i, J. S. Ladislaw, A. E. Dulcey, V. Percec, F. C. De Schryver, S. De Feyter, *J. Am. Chem. Soc.* **2006**, *128*, 317 – 325.
[29] S. M. Barlow, R. Raval, *Surf. Sci. Rep.* **2003**, *50*, 201 – 341.
[30] K. E. Plass, A. L. Grzesiak, A. J. Matzger, *Acc. Chem. Res.* **2007**, *40*, 287 – 293.
[31] Interestingly, the 2D stereochemistry of chiral (*S*)-OPV4T is not affected by the chiral nature of the solvent when experiments are performed in (*R*)- or (*S*)-1-phenyl-1-octanol.
[32] See Supporting Information.

